

Reaction $^{15}\text{N}(t,p)^{17}\text{N}$

H. T. Fortune, G. E. Moore,* L. Bland, M. E. Cobern,[†] S. Mordechai,[‡] and R. Middleton
Physics Department, University of Pennsylvania, Philadelphia, Pennsylvania 19104

R. D. Lawson

Argonne National Laboratory, Argonne, Illinois 60439

(Received 8 June 1979)

In $^{15}\text{N}(t,p)$, at $E_t = 15$ MeV, 19 angular distributions were measured for levels up to 7 MeV in excitation. Comparison with distorted-wave Born-approximation calculations allows extraction of L values for most of them. Two different simple shell model calculations are presented for the 2p-1h states and compared with the data.

NUCLEAR REACTIONS $^{15}\text{N}(t,p)$, $E = 15.0$ MeV; measured $\sigma(E_p, \theta)$. Enriched gas target. DWBA analysis. ^{17}N levels deduced L , π , J . Comparison with shell model.

I. INTRODUCTION

A study¹ of the reaction $^{15}\text{N}(t,p)$ has located in ^{17}N a number of two-particle - one-hole (2p-1h) states that are described predominantly as two sd -shell neutrons coupled to the ^{15}N ground state. A comparison of experimental angular distributions with those obtained for $^{16}\text{O}(t,p)$ gave results that were reasonably consistent with weak coupling. A more quantitative analysis requires the use of distorted-wave Born-approximation (DWBA) calculations and microscopic wave functions. The present paper reports the results of such an analysis and also presents data for several additional states.

II. EXPERIMENTAL PROCEDURE

A triton beam was obtained from a cesium negative ion source² and was accelerated to 15 MeV in the University of Pennsylvania FN tandem Van de Graaff accelerator. A closed, rotating gas cell³ with a $230 \mu\text{g}/\text{cm}^2$ aluminum window was used to contain the ^{15}N target gas at a pressure of 30 ± 1 Torr. The ^{15}N gas enrichment was 99%. The ^{15}N gas pressure was monitored indirectly during data collection by measuring the elastic scattering count rate in a solid state detector. Outgoing protons were momentum analyzed in a multiangle spectrograph and detected in nuclear emulsions after passing through Mylar absorber foils that stopped all heavier particles. Data were recorded in 7.5° intervals beginning at a lab angle of 7.5° . Absolute cross sections were measured to an accuracy of 10% using the known gas cell geometry, gas pressure, and integrated beam current.

A proton spectrum obtained at 7.5° is shown in

Fig. 1. The experimental resolution is 20 keV full width at half maximum (FWHM). Peaks arising from the $^{15}\text{N}(t,p)^{17}\text{N}$ reaction are numbered consecutively beginning with 0 for the ground state of ^{17}N . The only impurity peak present arises from the (t,p) reaction on the hydrogen impurity in the target. Excitation energies were obtained from measured peak positions at ten angles and averaged to get the results listed in Table I. Agreement with values from the literature⁴ is good. Most of the levels below 5 MeV in ^{17}N now have unique or probable J^π assignments.^{1,4} Positive-parity states (levels 2 and 4 at 1.85 and 2.53 MeV, respectively) are quite weak, as expected from their dominant 3p-2h structure. Most of the other levels have negative parity. Angular distributions for all states up to 7 MeV are displayed in Figs. 2 - 5.

III. ANALYSIS

Theoretical angular distributions were calculated with the microscopic two-nucleon transfer option of the code DWUCK⁵ using the same optical model parameters (Table II) as employed previously^{6,7,8} for $^{12,14}\text{C}(t,p)^{14,16}\text{C}$. Two different models have been used to describe the low-lying negative parity states in ^{17}N . In the first, we assume that the two valence neutrons are restricted to the $(1d_{5/2}, 2s_{1/2})$ model space and that the valence proton hole is in the $1p_{1/2}$ orbital. Empirical matrix elements describing the interaction between the valence neutrons were taken from the work of Lawson, Serduke, and Fortune⁹; in this paper we have used the constrained Π values given in Table VII of LSF. Unlike the situation in ^{18}O , we do not expect in ^{17}N any low-lying four-particle three-hole intruder

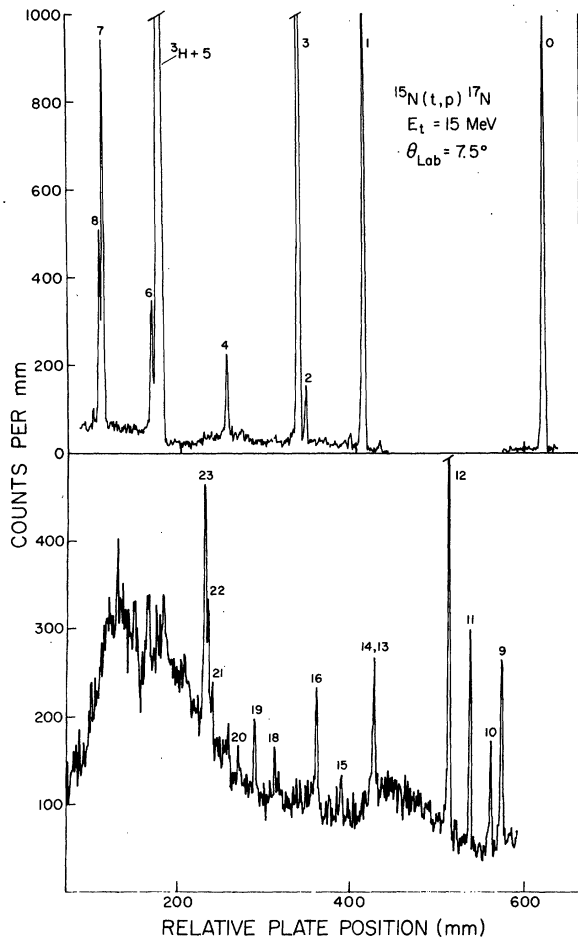


FIG. 1. Spectrum of the $^{15}\text{N}(t,p)^{17}\text{N}$ reaction at a bombarding energy of 15 MeV and a laboratory angle of 7.5° . Peaks are labeled numerically beginning with 0 for the ^{17}N ground state. Excitation energies are listed in Table I.

states in which the four particles have a “ ^{20}Ne -like” structure because this would require excitation of a proton out of the $p_{3/2}$ orbit. Such states in ^{17}N would lie many MeV above the $2p$ - $1h$ states. The single-particle and single-hole energies were obtained from the binding-energy tables of Wapstra and Bos¹⁰ and the spectrum⁴ of the single-particle nucleus ^{17}O ; values for these energies are listed in Table III.

Once the single-particle and single-hole energies are known the residual interaction between the $p_{1/2}$ -proton hole and the $s_{1/2}$ or $d_{5/2}$ neutron can be obtained from the spectrum of ^{16}N . If we assume that the 2^- ground state of ^{16}N corresponds to the configuration $[(\pi p_{1/2})^{-1} \times (\nu d_{5/2})_2]$ it follows that the diagonal matrix element E_2 of the residual interaction in this state is given by

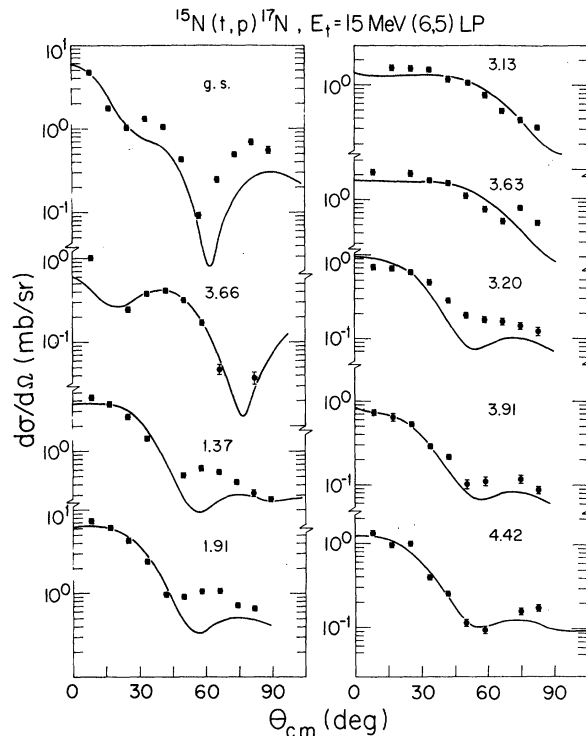


FIG. 2. Angular distributions and DWBA curves for predominantly $2p$ - $1h$ states. Normalization factors are given in Table IV, and theoretical wave functions in Table III.

$$\epsilon_p^{-1} + \epsilon_d + E_2 = -[E_B(^{16}\text{N}) - E_B(^{16}\text{O})],$$

where $E_B(A)$ is the binding energy of the ground state of the nucleus A . In a similar way the energies of the 0^- , 1^- , and 3^- states in ^{16}N provide us with the other necessary interaction energies and these are listed in Table III. When the results of Table III and the constrained II ($1d_{5/2}$, $2s_{1/2}$) matrix elements of LSF are used, the wave functions and excitation energies listed in Table IV under the heading LP are obtained.

In the harmonic oscillator approximation the probability of $L=2$ (t,p) transfer involving a pair of ($1d$, $2s$)-shell nucleons is in the ratio 1:0.667:0.229 when the pair involved is ($1d_{5/2}$, $2s_{1/2}$), ($1d_{3/2}$, $2s_{1/2}$), or ($1d_{5/2}$)², respectively. Consequently, a small component of ($1d_{3/2}$, $2s_{1/2}$)₂ in the 2^+ wave functions could substantially affect the calculated (t,p) cross sections to the $J^\pi = \frac{3}{2}^-$ and $\frac{5}{2}^-$ levels in ^{17}N . To estimate the effect of such a component in these states we have redone the shell-model calculation in a model space that allows at most one neutron in the $1d_{3/2}$ orbital. Again the constrained II matrix elements of LSF have been used and for simplicity we have as-

TABLE I. Results of the reaction $^{15}\text{N}(t, p) ^{17}\text{N}$.

Literature ^a			Present				Remarks
E_x (keV)	J^π	Level No.	E_x (keV)	J^π	$\left(\frac{d\sigma}{d\Omega}\right)_{\max}$ (mb/sr)	L	
0.0	$\frac{1}{2}^-$	0	0.0	$\frac{1}{2}^-$	4.8	0	
1373.9 ± 0.3	$\frac{3}{2}^-$	1	1372 ± 6	$\frac{3}{2}^-$	4.4	2	
1849.6 ± 0.3	$\frac{1}{2}^+$	2	1851 ± 4	$\frac{1}{2}^+$	0.37	1	
1906.8 ± 0.3	$\frac{5}{2}^-$	3	1909 ± 3	$\frac{5}{2}^-$	7.3	2	
2526.0 ± 0.5	$\frac{7}{2}^+$	4	2524 ± 4	$\frac{7}{2}^+$	0.60	3	
3128.9 ± 0.5	$\frac{7}{2}^{(-)}$	5	3127 ± 6	$\frac{7}{2}^-$	1.8	4	
3204.2 ± 0.9	$\frac{3}{2}^-$	6	3201 ± 5	$\frac{3}{2}^-$	0.72	2	
3628.7 ± 0.7	$(\frac{7}{2}, \frac{3}{2})^-$	7	3625 ± 6	$\frac{9}{2}^-$	2.1	4	
3663 ± 4	$(\frac{1}{2}, \frac{3}{2})^-$	8	3664 ± 6	$\frac{1}{2}^-$	1.0	0	
3906 ± 2	$\leq \frac{7}{2}$	9	3906 ± 5	$(\frac{3}{2}, \frac{5}{2})^-$	0.73	2	
4006 ± 2	$(\frac{3}{2})$	10	4011 ± 6	$(\frac{1}{2}, \frac{3}{2})^+$	0.33	(1)	
4208 ± 3	$\leq \frac{5}{2}$	11	4213 ± 6	$(\frac{7}{2}, \frac{5}{2})^+$	0.61	3	$J^\pi = \frac{5}{2}^+$
4415 ± 3	$\leq \frac{7}{2}$	12	4420 ± 7	$(\frac{3}{2}, \frac{5}{2})^-$	1.2	2	
5170 ± 2	$(\frac{7}{2}, \frac{3}{2})^+$	13	5179 ± 4		0.59	5	Probably $\frac{3}{2}^+$
5195 ± 3	$(\frac{1}{2}, \frac{5}{2})^+$	14				1	Probably $(\frac{1}{2}, \frac{3}{2})^+$
5514 ± 3	$(\frac{3}{2})^b$	15	5517 ± 6		0.21	(2)	
5770 ± 3	$\leq \frac{7}{2}$	16	5780 ± 6		0.46	(1)	
6080 ± 30		17	...				Not observed
6240 ± 25		18	6233 ± 8		0.32	(2)	
6430 ± 30		19	6449 ± 3		0.21	(4, 5)	
6610 ± 25		20	6627 ± 30				Weak
...		21	6938 ± 15				
6990 ± 20	b	22	6981 ± 20		1.2	(3, 4)	
		23	7013 ± 22				

^a Ref. 4.^b Probably $\frac{3}{2}^-$ from $^{18}\text{O}(d, ^3\text{He})$ (Ref. 11).

sumed that the $(\pi p_{1/2}^{-1})$ -neutron interaction can be taken into account by a change in the single-particle neutron energies. Thus

$$\begin{aligned} \epsilon_d &= \epsilon_{d_{5/2}} = -4.143 + \left(\frac{1}{12}\right) \sum_J (2J+1) E_J \\ &\quad \times (p_{1/2}^{-1} d_{5/2}; p_{1/2}^{-1} d_{5/2}), \\ \epsilon_s &= -3.272 + \left(\frac{1}{4}\right) \sum_J (2J+1) E_J (p_{1/2}^{-1} s_{1/2}; p_{1/2}^{-1} s_{1/2}), \\ \epsilon_{d_{3/2}} &= -4.143 + 5.08 \\ &\quad + \left(\frac{1}{12}\right) \sum_J (2J+1) E_J (p_{1/2}^{-1} d_{3/2}; p_{1/2}^{-1} d_{3/2}), \end{aligned} \quad (1)$$

where the E_J are given in Table III. We have also assumed that the average interaction between the $d_{3/2}$ neutron and $\pi p_{1/2}$ hole is the same as that between the $d_{5/2}$ neutron and $\pi p_{1/2}$ hole. The wave functions for the $J^\pi = \frac{1}{2}^-$ states obtained in this way are identical to those of the previous calculation since, if the two neutrons couple to zero spin, the interaction gives only a change in the single-particle energies. On the other hand, for $J \neq \frac{1}{2}$ this is only an approximation. In this approximation, states with $J = J_{2n} \pm \frac{1}{2}$ are degenerate doublets, since the model does not distinguish whether the proton spin is parallel or antiparallel to the angular momentum of the two neutrons. The energies and wave functions that result from this approximation are listed in Table IV under the la-

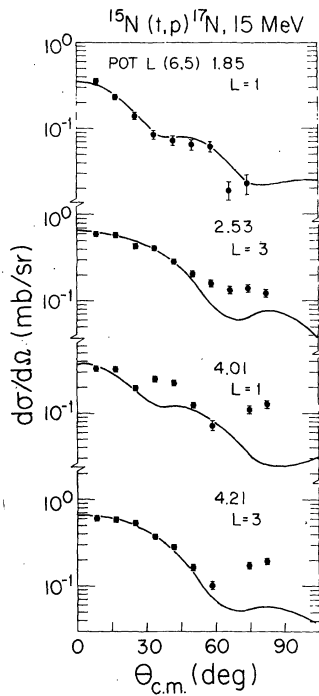


FIG. 3. Angular distributions and fits for additional levels below 5 MeV excitation.

bel LSF.

Both calculations predict the $\frac{3}{2}^-$ second excited state to be much too high. We return to this point below. The two sets of wave functions are very similar, except for the fact that the LP calculation splits the degeneracy.

Both sets of wave functions were then used as input in the DWBA calculations, producing the results displayed in Fig. 2. The curves have been arbitrarily normalized to the data, yielding the normalization factors N listed in Table V, where

$$\sigma_{\text{exp}}(\theta) = N \frac{(2J_f + 1)}{(2J_i + 1)} \frac{\sigma_{\text{DW}}(\theta)}{2L + 1}$$

For the $\frac{1}{2}^-$ states, the DWBA curve underpredicts the second maximum for the g.s. and overpredicts it (relative to more forward angles) for the 3.66-MeV level. Such effects have been ob-

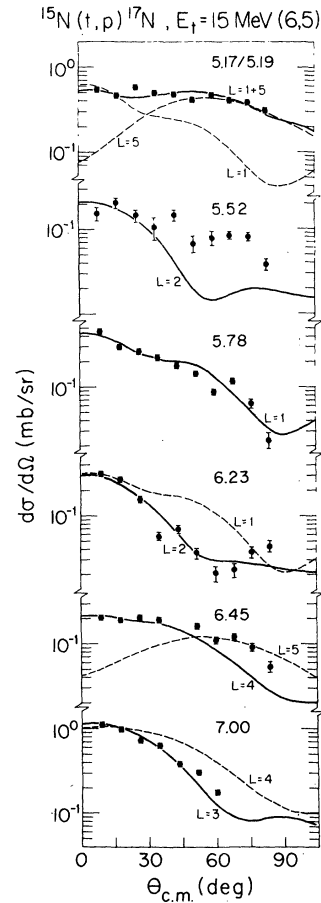


FIG. 4. Angular distributions for levels above 5 MeV excitation, compared with a variety of DWBA curves.

served previously^{7,8}, i.e., DWBA fails to account for the Q dependence of $L=0$ shapes as the Q value becomes quite negative. The two sets of wave functions are virtually identical for the $\frac{1}{2}^-$ states, resulting in nearly equal N values. For other states, the magnitudes differ somewhat in a few cases, but the angular-distribution shapes from the two sets of wave functions are identical.

For the $\frac{3}{2}^-$ levels, the LP calculation ignores the $d_{3/2} s_{1/2}$ and $d_{5/2} d_{3/2}$ components, but they are small in LSF. (The majority of these two configurations lies very much higher in excitation.) However,

TABLE II. Optical-model parameters (Ref. 6). Strengths in MeV, lengths in fm.

Channel	Label	V_0	$r_0 = r_{s0}$	$a = a_{s0}$	W	$W' = 4W_D$	r'_0	a'	$V_{s.o.}$
$^{15}\text{N}+t$	6	130	1.29	0.58	18.9	0	1.37	0.96	0
$^{17}\text{N}+p$	5	60	1.13	0.57	0	34.2	1.13	0.50	5.5
$^{15}\text{N}+n$...		1.26	0.60					$\lambda = 25$

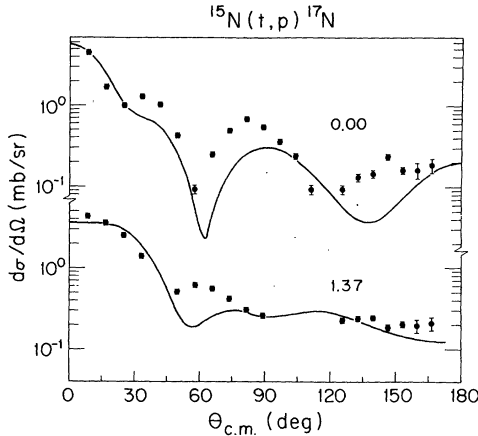


FIG. 5. Full angular distributions for two states with DWBA curves.

for the first $\frac{3}{2}^-$ state the theoretical cross section calculated with the LP amplitudes is about 30% smaller than that calculated with LSF. This comes about partly by neglect of the two above configurations, but also because LP contains less $1d_{5/2}2s_{1/2}$ in the first $\frac{3}{2}^-$ level than does LSF, and this is the most important term for the (t, p) cross section. The LP and LSF cross sections for the second $\frac{3}{2}^-$ state are very nearly equal.

The above remarks also hold for the $\frac{5}{2}^-$ levels, but here we have an additional difference, viz., in LP the mixing in of the configuration $[(1d_{5/2})(2s_{1/2})]_{3+}$ which is ignored in LSF. Thus LP allows the population in (t, p) of three $\frac{5}{2}^-$ states, whereas only two are allowed in LSF. Experimentally, three are seen, but the mixing between the upper two appears to be somewhat stronger than calculated in LP.

For the $\frac{7}{2}^-$ and $\frac{9}{2}^-$ levels, the only essential difference is the inclusion of the $1d_{5/2}1d_{3/2}$ configuration in LSF. This term, though small, makes a large contribution to the cross section.

Overall, the LP wave functions appear to more adequately reproduce the excitation energies and LSF the (t, p) strengths. Presumably, inclusion in LP of the extra configurations would fix the cross sections without seriously affecting the excitation energies.

The overall normalization factor N is expected^{7,8} to be about 300, with an uncertainty of about a factor of 2 in both directions. Most of our results fall within this range. It thus appears that even with reasonably simple wave functions, it is possible to predict absolute (t, p) cross sections to within a factor of 2. It is unlikely that the availability of more complicated wave functions will significantly improve the situation.

TABLE III. Energies used in the LP calculations.

Single-particle energies		
Configuration	Energy (MeV)	
$\pi(1p_{1/2})^{-1}$	12.128	
$\nu(1d_{5/2})$	-4.143	
$\nu(2s_{1/2})$	-3.272	
Two-body interactions		
Configuration	J^π	Energy (MeV)
$p^{-1}s; p^{-1}s$	0^-	0.900
$p^{-1}s; p^{-1}s$	1^-	1.178
$p^{-1}d; p^{-1}d$	2^-	1.651
$p^{-1}d; p^{-1}d$	3^-	1.948

We return now to the question of the excitation energy of the first $\frac{3}{2}^-$ state. The calculated excitation energies of both $\frac{1}{2}^-$ and lowest $\frac{7}{2}^-$ and $\frac{9}{2}^-$ states are in satisfactory agreement with experiment. Furthermore, the predicted binding energy of the $\frac{1}{2}^-$ ground state of ^{17}N relative to ^{16}O is also quite good—3.600 MeV compared to the experimental value of 3.753 MeV. On the other hand, the lowest $\frac{3}{2}^-$ and $\frac{5}{2}^-$ states are predicted at too high an excitation energy. For the former, this is consistent with the fact that this state is seen quite strongly in the $^{18}\text{O}(d, ^3\text{He})^{17}\text{N}$ reaction,¹¹ with $C^2S = 0.38$. Thus there is about a 10% admixture of $p_{3/2}^{-1}$ in the first $\frac{3}{2}^-$ level. If one assumes that the $p_{3/2}$ -hole state lies 6.3 MeV above the $p_{1/2}$ (as it does in ^{15}N) a 10% admixture of $p_{3/2}^{-1}$ would imply an off diagonal matrix element between the $p_{3/2}$ - and $p_{1/2}$ -hole states of 2.36 MeV and this would lower the energy of the first $\frac{3}{2}^-$ state by about 800 keV—bringing its predicted position close to that observed.

Below 5 MeV, the only levels not discussed so far are those (see Fig. 3) at 1.85, 2.53, 4.01, and 4.21 MeV. Of these the first is known to have $J^\pi = \frac{1}{2}^+$, the second has positive parity, probably with $J = \frac{5}{2}$, the third has a tentative $J = \frac{3}{2}$ assignment, and the fourth $J \leq \frac{5}{2}$. The lowest positive-parity configuration expected in ^{17}N is

$$[(sd)_{T=1/2}^3 \times (1p)_{T=1}^{-2}]_{T=3/2},$$

i.e., in weak coupling $[^{19}\text{F} \otimes ^{14}\text{C}]$. A simple calculation shows that the observed energies are consistent with this description of the states. From the work of Bansal and French¹² it follows that the excitation energies of the $[^{19}\text{F}(J^*) \otimes ^{14}\text{C}]_{J, T=3/2}$ states are

$$E_J = -\{E_B[^{19}\text{F}(J^*) + E_B(^{14}\text{C}) - E_B(^{16}\text{O}) - E_B(^{17}\text{N})\} + 6a + b/2 + 2\epsilon_c, \quad (2)$$

where $E_B[^{19}\text{F}(J^*)]$ is the binding energy of the

TABLE IV. Excitation energies and wave functions of lowest 2p-1h states in ^{17}N .

J^π	E_x (MeV)		Type	Amplitudes ^b				
	Exp ^a	Th		d_0^2p	s_0^2p	$(dd')_2p$	$(d's)_2p$	
$\frac{1}{2}^-$	0.0	0.0	LSF	0.845	0.536			
		0.0	LP	0.840	0.543			
$\frac{1}{2}^-$	3.66	3.77	LSF	0.536	-0.845			
		3.77	LP	0.543	-0.840			
				d_2^2p	$(ds)_2p$	$(dd')_2p$	$(d's)_2p$	
$\frac{3}{2}^-$	1.37	2.47	LSF	0.787	+0.572	0.054	-0.226	
		2.37	LP	0.857	0.514			
$\frac{3}{2}^-$	3.20	3.81	LSF	-0.599	0.798	0.030	-0.059	
		3.71	LP	-0.514	0.857			
				d_2^2p	$(ds)_2p$	$(dd')_2p$	$(d's)_2p$	$(ds)_3p$
$\frac{5}{2}^-$	1.91	2.47	LSF	0.787	0.572	0.054	-0.226	
		2.59	LP	0.839	0.541			
$\frac{5}{2}^-$	3.91	3.81	LSF	-0.599	0.798	0.030	-0.059	
		3.85	LP	-0.533	0.798			
$\frac{5}{2}^-$	4.42	4.50	LSF	...			-0.280	
		4.44	LP	-0.107	0.265		1.0	
				d_4^2p	$(dd')_4p$	$(ds)_3p$	0.958	
$\frac{7}{2}^-$	3.13	3.53	LSF	0.989	0.148			
		3.42	LP	1.0				
$\frac{7}{2}^-$	(4.21)	4.50	LSF			1.0		
		4.84	LP			1.0		
				d_4^2p	$(dd')_4p$			
$\frac{9}{2}^-$	3.63	3.53	LSF	0.989	0.148			
		3.87	LP	1.0				

^a Ref. 4.^b d, s, d' , and p denote $1d_{5/2}, 2s_{1/2}, 1d_{3/2}$, and $1p_{1/2}^{-1}$, respectively. Subscripts give J for the pair of sd -shell nucleons.

$^{19}\text{F}(sd)^3$ state with spin J and the other binding energies are for the nuclear ground states. The interaction strengths a and b are the monopole isoscalar and isotensor particle-hole interactions and ϵ_c is the particle-hole Coulomb interaction energy. According to Zamick,¹³ a reasonable fit to the particle-hole data in this region of nuclei can be obtained if

$$\begin{aligned} a &= 0.34 \text{ MeV}, \\ b &= 4.91 \text{ MeV}, \\ \epsilon_c &= -0.5 \text{ MeV}. \end{aligned} \quad (3)$$

When these values are inserted into Eq. (2) one predicts the lowest positive-parity states in ^{17}N to lie at excitation energies of

$$\begin{aligned} E_x(\frac{1}{2}^+) &= 1.79 \text{ MeV}, \\ E_x(\frac{5}{2}^+) &= 1.99 \text{ MeV}, \\ E_x(\frac{3}{2}^+) &= 3.34 \text{ MeV}. \end{aligned}$$

The energy of the $\frac{1}{2}^+$ state is quite well reproduced by the simple model whereas that of the $\frac{5}{2}^+$ state is too low. However, the parameters a and b of Eq. (3) are independent of J only if the structure of the $(sd)^3$ states is the same for different values of J . Consequently it is not surprising that the predicted excitation energy is better for one of these states than for the other.

If the dominant configuration of the first $\frac{5}{2}^+$ and $\frac{3}{2}^+$ states in ^{19}F is the same, then on the basis of the weak-coupling model the energy difference between these two states in ^{17}N should be the same as observed in ^{19}F —, i.e., if the 2.53-MeV state in ^{17}N is the $\frac{5}{2}^+$ level, then the $\frac{3}{2}^+$ state should lie at

$$E_x(\frac{3}{2}^+) = 2.53 + 1.36 = 3.89 \text{ MeV},$$

which is quite close to the observed 4.01-MeV state.

The next positive-parity state that arises from [$^{19}\text{F}(J^+) \otimes ^{14}\text{C}$] would be the $\frac{9}{2}^+$ level, and on the ba-

TABLE V. Absolute normalization factors N , where $\sigma_{\text{exp}} = N[(2J_f + 1)/(2J_i + 1)][\sigma_{\text{DW}}/(2J + 1)]$.

E_x	J^π	N	
		LSF	LP
0.0	$\frac{1}{2}^-$	170	175
1.37	$\frac{3}{2}^-$	175	275
1.91	$\frac{5}{2}^-$	200	292
3.13	$\frac{7}{2}^-$	338	451
3.20	$\frac{3}{2}^-$	100	108
3.63	$\frac{3}{2}^-$	306	405
3.66	$\frac{1}{2}^-$	160	180
3.91	$(\frac{5}{2}^-)$	67	72
4.42	$(\frac{5}{2}^-)$...	800

sis of Eqs. (2) and (3) its expected excitation energy would be $1.79 + 2.78 = 4.57$ MeV. This is not too far from the observed state at 4.21 MeV. However, if the suggested⁴ limit $J \leq \frac{5}{2}$ for the observed state is correct, one must look for some other explanation for it. If one evaluates the energy associated with the configuration

$$\Psi = [(ds)_{J_p=5/2, T_p=3/2} \otimes (p)_{J_h=0, T_h=1}^{-2}]_{J=5/2, T=3/2} \quad (4)$$

one finds, by use of Eq. (3), that such a state is predicted to lie at an excitation energy of 3.24 MeV in ^{17}N . Thus both the spin and excitation energy of the 4.21-MeV state would be consistent with this configuration. However, although the weak-coupling model is quite successful in predicting the energies of states with isospin $T = T_p + T_h$ [i.e., the stretched isospin configuration which for ^{17}N would correspond to $[(sd)_{T=1/2}^3 \times (p)_{T=1}^{-2}]_{T=3/2}$], states with $T < T_p + T_h$ are always predicted to lie at too low an excitation energy when the number of holes or number of particles is greater than one.¹⁴ Consequently we cannot state with any degree of confidence that the 4.21-MeV state is the $J^\pi = \frac{5}{2}^+$ level of Eq. (4).

Angular distributions for these four states are presented in Fig. 3, where they are compared with DWBA curves calculated assuming pure configurations with $L = 1, 3, 1,$ and 3 , respectively. The fits are reasonable, suggesting that if previous limits are correct, then $J^\pi(4.01) = \frac{3}{2}^+$ and $J^\pi(4.21) = \frac{5}{2}^+$. But if this identification is correct, then a $\frac{7}{2}^-$ state of the form $[(1d_{5/2})(2s_{1/2})]_{3^+} \otimes (1p_{1/2})^{-1}$, which is predicted near 4.8 MeV, is still missing. Such a state can be made in (t, p) via sequential transfer. In earlier work^{7,8}, 3^+ states have possessed angular distributions whose shapes were very similar to $L = 3$ DWBA curves. We may have

the same effect here. In fact, the cross section for the 4.21-MeV state is consistent with such a process [by comparison with $^{14}\text{C}(t, p)^{16}\text{C}(3^+)$]. However, as noted above, the compilation lists $J \leq \frac{5}{2}$ for the 4.21-MeV level.

Above 5 MeV in excitation the situation is less clear, but we observe six levels (or groups of levels) sufficiently strong to allow extraction of angular distributions. They are displayed in Fig. 4. States at 5.17 and 5.19 MeV have J^π restrictions of $(\frac{7}{2}, \frac{9}{2})^+$ and $(\frac{1}{2}, \frac{5}{2})^+$, respectively. The combined angular distribution appears to be reasonably well fitted by a sum of $L = 1 + 5$ curves. This result is consistent with the previous information, but would require $J^\pi = \frac{9}{2}^+$ for the lower member and $J^\pi = (\frac{1}{2} \text{ or } \frac{3}{2})^+$ for the upper. The splitting between the $\frac{5}{2}^+$ and $\frac{9}{2}^+$ levels of ^{17}N is then 2.64 MeV, very close to the splitting of 2.58 MeV in ^{19}F .

The state at 5.52 MeV is quite weak and has a nondescript angular distribution. An $L = (2)$ assignment is very tentative, but consistent with a probable $(\frac{3}{2})^-$ assignment from $^{11}\text{O}(d, ^3\text{He})$. The 5.78-MeV angular distribution is very well fitted by an $L = 1$ DWBA curve, implying $J^\pi = \frac{1}{2}^+$ or $\frac{3}{2}^+$. Previous information⁴ only restricted $J \leq \frac{7}{2}$. The 6.23-MeV level appears to have an $L = 2$ angular distribution, implying $J^\pi = \frac{3}{2}^-$ or $\frac{5}{2}^-$. No previous data are available for the J^π of this or higher states.

The angular distribution for the 6.45-MeV state is not well fitted by any single L value, but appears to require both $L = 4$ and 5 , suggesting the presence of at least two states.

The angular distribution labeled "7.00" contains contributions from at least three states, at 6.94, 6.98, and 7.01 MeV. However, the highest of the three appears to dominate and to have an $L = 3$ shape. One of these states could be the probable $(\frac{3}{2})^-$ level observed¹¹ at 6.99 MeV in $^{18}\text{O}(d, ^3\text{He})$.

The fits to the angular distribution shapes are not as good as those encountered^{7,8} in $^{12,14}\text{C}(t, p)^{14,16}\text{C}$, but they are still sufficient to allow extraction of L values and relative strengths for most states. We have investigated a number of different sets of optical-model parameters, but we find no set which simultaneously gives better fits for $L = 0, 2,$ and 4 . It may be that processes other than direct simultaneous $2n$ transfer are present. We have investigated the presence of compound-nuclear processes by obtaining data at extreme backward angles for two states. These are displayed in Fig. 5 where they are compared with DWBA curves. It is observed that the back angle cross section is only 0.05–0.10 of that at forward angles, so that CN effects can probably be neglected in the present case, though perhaps not for states with significantly smaller cross sections.

It may be that inelastic and/or sequential two-step mechanisms mentioned above are important. Calculations of such processes are underway, but preliminary results indicate negligible contribu-

tion for most of the states discussed above.

We acknowledge financial support from the National Science Foundation and the U.S. Department of Energy.

*Present address: Analytic Services Inc., 400 Army Nave Drive, Arlington, Virginia 22202.

†Present address: N. L. Petroleum Services, P. O. Box 1473, Houston, Texas 77001.

‡Present address: Department of Physics, Ben-Gurion Univ. of The Negev, Beer-Sheva, Israel (P. O. Box 2053).

¹G. E. Moore *et al.*, Phys. Lett. 76B, 192 (1978).

²R. Middleton, C. T. Adams, and R. V. Kollarits, Nucl. Instrum. Methods 151, 41 (1978).

³J. D. Garrett, Ph. D. thesis, Univ. of Penna., 1972 (unpublished).

⁴F. Ajzenberg-Selove, Nucl. Phys. A281, 1 (1977).

⁵P. D. Kunz (private communication).

⁶P. W. Keaton *et al.*, Nucl. Phys. A179, 561 (1972).

⁷H. T. Fortune *et al.*, Phys. Lett. 70B, 408 (1977).

⁸S. Mordechai *et al.*, Nucl. Phys. A301, 463 (1978).

⁹R. D. Lawson, F. J. Serduke, and H. T. Fortune, Phys. Rev. C 14, 1245 (1976).

¹⁰A. H. Wapstra and K. Bos, At. Data Nucl. Data Tables 19, 177 (1977).

¹¹G. Mairle *et al.*, Nucl. Phys. A280, 97 (1977).

¹²R. K. Bansal and J. B. French, Phys. Lett. 11, 145 (1964).

¹³L. Zamick, Phys. Lett. 19, 580 (1965).

¹⁴R. Sherr, R. Kouzes, and R. del Vecchio, Phys. Lett. 52B, 401 (1974).